JGR Oceans

RESEARCH ARTICLE
10.1029/2024JC021668

Quantifying the Potential Predictability of Arctic Marine Primary Production

Courtney M. Payne[1,2], Nicole S. Lovenduski[1], Marika M. Holland[2], Kristen M. Krumhardt[2], and Alice K. DuVivier[2]

[1]Department of Atmospheric and Oceanic Sciences and Institute of Arctic and Alpine Research, University of Colorado, Boulder, CO, USA, [2]National Center for Atmospheric Research Climate and Global Dynamics Lab, Boulder, CO, USA

Key Points:

- Arctic phytoplankton net primary production can be predicted for multiple years, largely due to the predictability of Arctic shelves
- This predictability is driven by ocean temperatures, which are an important limit on phytoplankton growth and maintain predictability
- Phytoplankton net primary production predictability in the Arctic may increase in the near future (2030s) relative to the 2010s

Supporting Information:

Supporting Information may be found in the online version of this article.

Correspondence to:

C. M. Payne,
courtney.payne-1@colorado.edu

Citation:

Payne, C. M., Lovenduski, N. S., Holland, M. M., Krumhardt, K. M., & DuVivier, A. K. (2025). Quantifying the potential predictability of Arctic marine primary production. *Journal of Geophysical Research: Oceans*, *130*, e2024JC021668. https://doi.org/10.1029/2024JC021668

Received 31 JUL 2024
Accepted 7 MAR 2025

Author Contributions:

Conceptualization: Courtney M. Payne, Nicole S. Lovenduski, Marika M. Holland, Kristen M. Krumhardt, Alice K. DuVivier
Data curation: Marika M. Holland
Formal analysis: Courtney M. Payne, Nicole S. Lovenduski, Marika M. Holland, Kristen M. Krumhardt, Alice K. DuVivier
Funding acquisition: Nicole S. Lovenduski
Investigation: Courtney M. Payne
Methodology: Courtney M. Payne, Nicole S. Lovenduski, Marika M. Holland, Kristen M. Krumhardt, Alice K. DuVivier
Resources: Marika M. Holland
Supervision: Nicole S. Lovenduski, Marika M. Holland, Kristen M. Krumhardt, Alice K. DuVivier
Validation: Courtney M. Payne
Visualization: Courtney M. Payne, Nicole S. Lovenduski, Marika M. Holland, Kristen M. Krumhardt, Alice K. DuVivier

Abstract Phytoplankton in the Arctic Ocean and sub-Arctic seas support a rich marine food web that sustains Indigenous communities as well as some of the world's largest fisheries. As sea ice retreat leads to further expansion of these fisheries, there is growing need for predictions of phytoplankton net primary production (NPP), which will likely allow better management of food resources in the region. Here, we use perfect model simulations of the Community Earth System Model version 2 (CESM2) to quantify short-term (month to 2 years) predictability of Arctic Ocean NPP. Our results indicate that NPP is potentially predictable during the most productive summer months for at least 2 years, largely due to the highly predictable Arctic shelves where fisheries in the Arctic are projected to expand. Sea surface temperatures, which are an important limitation on phytoplankton growth and also are predictable for multiple years, are the most important physical driver of this predictability. Finally, we find that the predictability of NPP in the 2030s is enhanced relative to the 2010s, indicating that the utility of these predictions may increase in the near future. This work indicates that operational forecasts using Earth system models may provide moderately skillful predictions of NPP in the Arctic, possibly aiding in the management of Arctic marine resources.

Plain Language Summary Phytoplankton form the base of the marine food web, supporting Indigenous communities and some of the world's largest fisheries in the Arctic Ocean and in sub-Arctic seas. As sea ice continues to retreat, fisheries are expected to expand in the Arctic, and predicting phytoplankton growth could allow us to better manage these fisheries. We used model simulations to investigate the upper limit in short-term phytoplankton productivity prediction and we found that phytoplankton can be predicted for at least 2 years, especially in the shallow continental shelves of the Arctic Ocean where fisheries are expected to expand. This predictability was largely provided by ocean temperatures, which control the rate of phytoplankton growth and can be predicted for multiple years. We also found that predictability in the 2030s was higher than in the 2010s, indicating that predictions may improve in the near future. This work demonstrates that models may provide useful predictions of NPP in the Arctic, aiding in the management of fisheries in the region.

1. Introduction

Marine phytoplankton comprise the base of the oceanic food web and mediate the global carbon (C) cycle by fixing inorganic C in the surface ocean and sequestering it at depth (Falkowski, 2012; Field et al., 1998; Volk & Hoffert, 1985). Although they account for only 1% of global photosynthetic biomass, phytoplankton generate nearly half of the world's net primary production, or NPP (Falkowski, 2012). Phytoplankton NPP is controlled by ocean temperatures and the availability of light and nutrients (Sigman & Hain, 2012) and can show substantial seasonal-to-interannual variability both globally and regionally (Elsworth et al., 2020, 2021; Krumhardt et al., 2017; Séférian et al., 2014), altering food availability for upper trophic level organisms and the efficacy of the biological C pump on short timescales.

In the Arctic Ocean, phytoplankton NPP forms the foundation of a diverse and dynamic food web. Satellite-based estimates indicate that Arctic phytoplankton fix ~500 Tg C yr^{-1} (Arrigo & Van Dijken, 2011, 2015) and that between 1998 and 2018, NPP increased by 57% (Lewis et al., 2020). This primary production supports large zooplankton communities (Ashjian et al., 2003; Ershova et al., 2015; Hopcroft et al., 2005; Mueter et al., 2021; Smidt, 1979), allowing the Arctic Ocean to serve as a critical feeding ground for both polar and migrating fish, marine mammals, and seabirds (Boertmann et al., 2004; Bradstreet & Cross, 1982; Hamilton et al., 2021; Joiris, 2011; Loeng et al., 2005; Logerwell et al., 2015; Munk, 2003; Rysgaard et al., 1999; Tsujii et al., 2016). While

Writing – original draft: Courtney M. Payne
Writing – review & editing: Courtney M. Payne, Nicole S. Lovenduski, Marika M. Holland, Kristen M. Krumhardt, Alice K. DuVivier

some of the world's largest fisheries are located in the sub-Arctic (Christiansen et al., 2014; Hollowed & Sundby, 2014), Arctic Ocean fisheries are largely small-scale (Tai et al., 2019; Zeller et al., 2011). However, these largely community-managed Arctic fisheries are a critical source of income for Indigenous communities and are key to cultural traditions and food sovereignty (Divine et al., 2021; Hoover et al., 2013; Lysenko & Schott, 2019).

Phytoplankton NPP in the Arctic Ocean is subject to large year-to-year variability and is projected to be impacted by long-term anthropogenic climate change. Arctic NPP exhibits substantial interannual variability, driven by diminishing sea ice cover and possibly by increases in nutrient inventories in the surface ocean (Arrigo & Van Dijken, 2015; Lewis et al., 2020). As a result of anthropogenic climate change, the Arctic has experienced dramatic increases in temperature and declines in sea ice extent (Beer et al., 2020; Holland & Bitz, 2003; Kwok, 2018; Meier & Stroeve, 2022; Rantanen et al., 2022; Screen & Simmonds, 2010; Timmermans & Labe, 2023), with consequences for phytoplankton species composition as well as the timing and magnitude of Arctic NPP (Ardyna et al., 2014; Arrigo et al., 2014; Arrigo & Van Dijken, 2015; Lewis et al., 2020; Li et al., 2009; Payne et al., 2024; Terhaar et al., 2020). Models estimate that Arctic Ocean phytoplankton NPP may increase by 2100 (Tagliabue et al., 2021; Vancoppenolle et al., 2013), though these projections are plagued by high uncertainty, largely due to uncertainty in future nutrient inventories (Carmack & Chapman, 2003; Crawford et al., 2020; McLaughlin & Carmack, 2010; Nummelin et al., 2015; Rainville & Woodgate, 2009; Tremblay et al., 2011; Zhang et al., 2004). Variability and changes to Arctic phytoplankton NPP have already coincided with changes in the fish species observed in the Arctic (Fossheim et al., 2015; Frainer et al., 2017), and fisheries and other marine food resources will likely be impacted in the near future as the open water area, length of the fishing season, and harvestable species are all projected to change (Christiansen et al., 2014; Tai et al., 2019; Wisz et al., 2015). Arctic marine resource management thus stands to benefit from advanced knowledge of NPP variations in a changing climate.

Using Earth system models (ESMs) that include a mathematical representation of primary and secondary producers in the ocean, several studies have demonstrated that variations in NPP can be predicted multiple years in advance (Frölicher et al., 2020; Krumhardt et al., 2020; Séférian et al., 2014; Yeager et al., 2018). A few studies have used ESMs to investigate multi-year predictability of NPP in polar regions, where variations in NPP are strongly tied to interannual variation in sea ice. Buchovecky et al. (2023) found that the spring bloom in the seasonally ice-covered Southern Ocean is potentially predictable more than 7 years in advance, and work by Fransner et al. (2023) demonstrated that phytoplankton abundance in the Barents Sea can be predicted up to 5 years in advance. While quite a few studies have investigated the potential seasonal predictability of Arctic sea ice (e.g., Blanchard-Wrigglesworth, Armour, et al., 2011; Blanchard-Wrigglesworth, Bitz, & Holland, 2011; Blanchard-Wrigglesworth & Bushuk, 2019; Bushuk et al., 2017; Holland et al., 2019; Lindsay et al., 2008; Merryfield et al., 2013), the seasonal predictability of NPP across the Arctic has not yet been explicitly explored. Given the utility of seasonal NPP forecasts for marine resource management (Brodie et al., 2023; Tommasi et al., 2017; Yeager et al., 2022) in a rapidly changing environment, quantifying the seasonal predictability of Arctic NPP and its evolution under anthropogenic climate change may prove critical to managing regional marine resources in the future.

This study investigates, for the first time, the potential near-term (month to 2 years) predictability of NPP in the Arctic Ocean and sub-Arctic seas and its evolution in a rapidly changing climate. We do this within the context of the Community Earth System Model and use "perfect model" ESM experiments to quantify the predictability of NPP, to evaluate differences in predictability between the 2010s and 2030s, and to identify the physical drivers of NPP predictability during these two periods. These two analysis periods are separated by two decades, allowing us to assess how substantial changes in Arctic climate may alter the predictability of phytoplankton productivity in the near future. We will demonstrate that NPP in the Arctic is potentially predictable on multi-year timescales and that much of this predictability is provided by the Arctic shelves, where fisheries are likely to expand substantially (Tai et al., 2019).

2. Methods

2.1. CESM

This analysis relies on simulations of the Community Earth System Model version 2 (CESM2), an ESM that includes atmosphere (the Community Atmosphere Model version 6; CAM6), ocean, sea ice, and terrestrial (Community Land Model version 5; CLM5) components run at 1° horizontal resolution (Danabasoglu

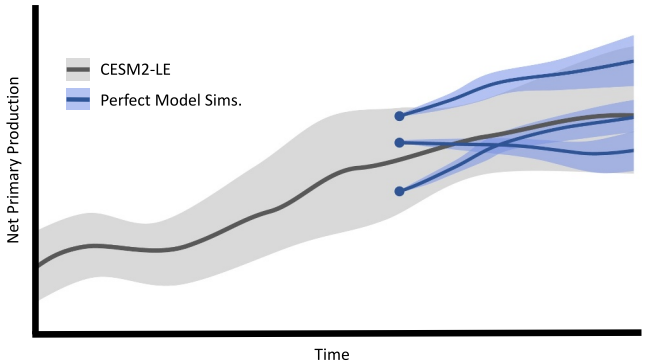

Figure 1. The mean and standard deviation of net primary production over time for the Community Earth System Model version 2 large ensemble (CESM2-LE; gray line and shading), which provides climatological variability, and for perfect model forecasts (blue lines and shading), initialized in 2010 and 2030.

et al., 2020). The ocean is simulated by the Parallel Ocean Program version 2 (POP2) and uses 60 vertical layers. Sea ice dynamics and thermodynamics are simulated using the CICE model (version 5.1.2; Hunke et al., 2017), which includes a sub-grid scale ice thickness distribution to represent the spatial heterogeneity of sea ice and calculates light availability for photosynthesis in grid cells with partial and full sea ice coverage (Long et al., 2015). CESM2 represents ocean biogeochemistry using the Marine Biogeochemistry Library (MARBL; Long et al., 2021), which is composed of three phytoplankton functional types (representing diatoms, diazotrophs, and picophytoplankton) and one generic zooplankton type and simulates the marine cycle of carbon, oxygen, and the nutrients nitrogen (N), phosphorus (P), silica (Si), and iron (Fe). CESM2 has been extensively evaluated with observational and reanalysis products (Danabasoglu et al., 2020; Long et al., 2021). While CESM2 captures the observed negative trends in 1979–2014 sea ice extent (DuVivier et al., 2020) and cloud cover over the Arctic Ocean (McIlhattan et al., 2020), it produces sea ice (DuVivier et al., 2020) and snow on ice (Webster et al., 2021) that is too thin, resulting in some inaccuracies in light limitation in ice-covered waters. Simulated sea surface temperatures demonstrate reasonable agreement with observations in the Arctic Ocean (Danabasoglu et al., 2020) and while modeled N concentrations are low in the sub-Arctic Pacific, they match observations well in the Arctic Ocean and other sub-Arctic regions (Long et al., 2021). Consequently, CESM2 has been found to replicate observed patterns of N and Fe limitation globally (Long et al., 2021). NPP produced by CESM2 for regions poleward of 50°N has not previously been explicitly evaluated against observations. Here, we compare monthly integrated 0–100 m NPP produced by 50 members of the CESM2 large ensemble (CESM2-LE; see details of these simulations below) to monthly NPP produced by an Arctic-specific algorithm (Lewis & Arrigo, 2020) as well as two global NPP algorithms, VGPM (Vertically Generalized Production Model; Behrenfeld & Falkowski, 1997) and CbPM (Carbon-based Production Model; Westberry et al., 2008). We present this evaluation for the 2005–2014 period.

2.2. Simulations

For this analysis, we use both the CESM2-LE (Rodgers et al., 2021) and a prediction ensemble composed of sets of ensemble simulations initialized from CESM2-LE simulations. We use 50 members of the large ensemble that are initialized in 1850 with a pre-industrial control simulation and are subsequently run for historical (1850–2014) and future (2015–2100) scenario periods using historical and SSP3-7.0 forcing protocols from the 6^{th} Coupled Model Intercomparison Project (CMIP6; Eyring et al., 2016). Ensemble members have identical prescribed forcing but differ due to a roundoff-level perturbation (10^{-14} K) in the initial air temperature and different initial ocean states. Consequently, the spread between ensemble members demonstrates the effect of internal climate variability (Deser et al., 2012). In addition to the CESM2-LE, we use a specialized set of "perfect model" forecasts. Five CESM2-LE ensemble members are randomly selected, and 15 forecast ensemble members are generated for each of these selections by initializing from the 2010 and 2030 coupled model state and perturbing air temperatures by 10^{-14} K (Figure 1 blue lines and shading). Prediction ensembles (15 members each for five initial states) are initialized on 1 January, 1 March, 1 May, 1 July, 1 September, and 1 November, yielding 75 forecast ensemble members for each initialization month. Predictability is subsequently quantified by comparing how these forecast ensemble simulations diverge from each other over time (Figure 1). These "perfect model" forecasts use the model to predict itself. While these experiments can be influenced by the climate biases of the underlying model, they do not depend on model skill. As such, these experiments provide a measure of potential predictability, rather than a measure of true forecast skill using an observational data set.

2.3. Analysis

We assess predictability across the Arctic Ocean and in sub-Arctic seas. We consider all ocean grid cells north of 50°N to be in the "Arctic Ocean". To evaluate regional predictability, we use Large Marine Ecosystems (LMEs; https://www.seaaroundus.org/; Figure 2a) and divide the Arctic into four regions—the Arctic shelves (>66.5°N and a grid cell depth of <1,000 m), Arctic deep ocean (>66.5°N, depth of >1,000 m), sub-Arctic shelves (50–66.5°N, depth of <1,000 m), and sub-Arctic deep ocean (50–66.5°N, depth of >1,000 m; Figure 2b). We compare

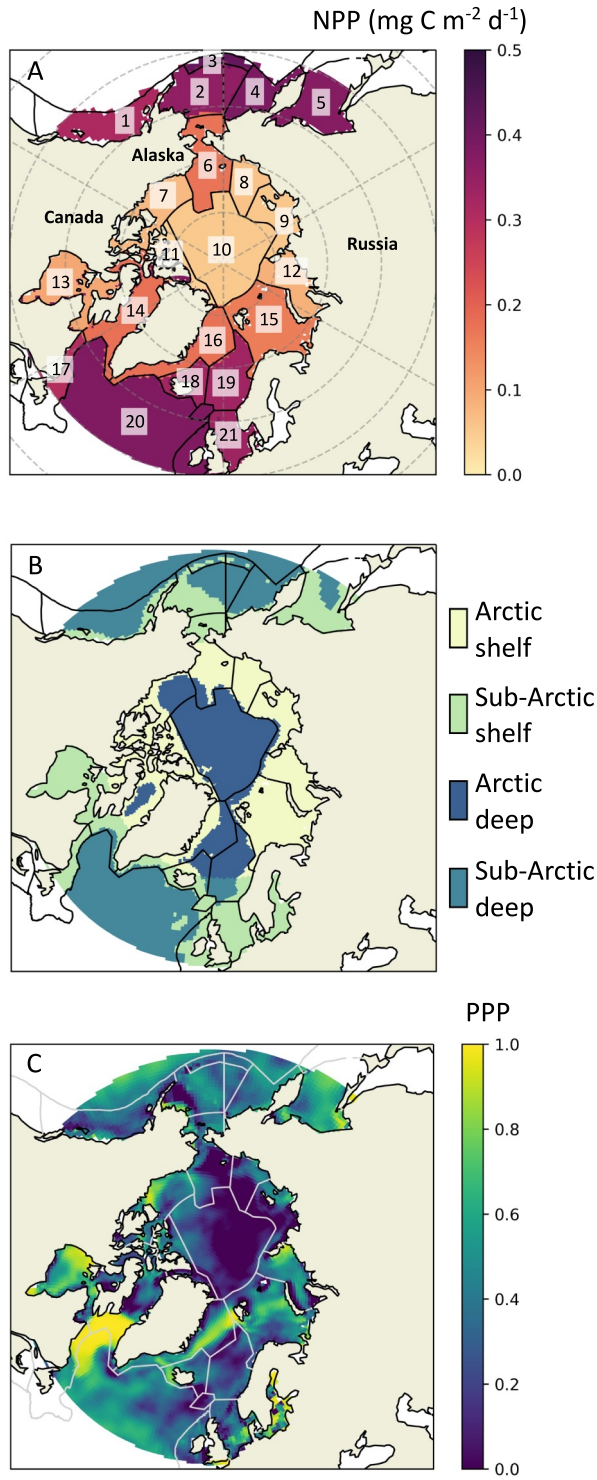

Figure 2. (a) Community Earth System Model version 2 Large Ensemble 2010–2012 annual mean NPP (mg C m^{-2} d^{-1}) for each large marine ecosystem (LME; https://www.seaaroundus.org/) in the Arctic Ocean (black lines). Labels indicate the boundaries of the (1) Gulf of Alaska, (2) West Bering Sea, (3) Aleutian Islands, (4) East Bering Sea, (5) Sea of Okhotsk, (6) North Bering and Chukchi Seas, (7) Beaufort Sea, (8) East Siberian Sea, (9) Laptev Sea, (10) central Arctic, (11) Canadian High Arctic and North Greenland, (12) Kara Sea, (13) Hudson Bay, (14) Canadian East Arctic and West Greenland, (15) Barents Sea, (16) Greenland Sea, (17) Newfoundland-Labrador Shelf, (18) Iceland Sea and Shelf, (19) Norwegian Sea, and (21) North Sea LMEs, as well as the (20) north Atlantic. (b) Study region, separated into Arctic (>66.5°N) and sub-Arctic (50–66.5°N) shelves (<1,000 m) and deep ocean (>1,000 m), with LME boundaries marked in black. (c) June 2010 mean Prognostic Potential Predictability (PPP) for each grid cell for perfect model experiments initialized 1 May 2010. LME boundaries are marked in gray.

variability across CESM2-LE members from 2010 to 2012 and 2030–2032 to variability across the perfect model experiment ensemble members for the same years. Because NPP is lognormally distributed, we calculate variance for ln(NPP) as in Campbell (1995).

We quantify prediction skill using the intra-ensemble Prognostic Potential Predictability (PPP; Pohlmann et al., 2004, Figure 2c), such that

$$PPP = 1\frac{\overline{\sigma^2}_{pme}}{\sigma^2_{clim}}, \quad (1)$$

where $\overline{\sigma^2}_{pme}$ represents the mean of the variability across the different initializations of the perfect model experiments and σ^2_{clim} represents the variability of the climatology, here the variability for the CESM2-LE simulations for 2010–2012 or 2030–2032. PPP is a commonly used metric for assessing predictability in idealized studies (e.g., Germe et al., 2014; Holland et al., 2011; Koenigk & Mikolajewicz, 2009; Pohlmann et al., 2004). It is typically used to quantify the upper limit of predictability, or the "predictability horizon" (Séférian et al., 2018). With the perfect model approach used here, there is not a specific state (e.g., from observations or a control run) that is being predicted. Instead, we seek to assess how rapidly the simulations lose the "memory" of the initial state that would allow for predictable conditions. PPP provides a simple but intuitive metric for this in that it measures the spread of ensemble members that are initialized with nearly identical conditions relative to the spread expected from internal variability. A PPP value of 1 amounts to perfect predictability, while a value less than 0 indicates that the variance among ensemble members is greater than that of the climatology, and thus that there is no predictive skill. In our analysis, negative PPP values could be attributed to either very low variance in both the climatology and the experimental ensemble sets or as a consequence of the relatively small sample size for the ensemble sets. Consequently, PPP values <0 are excluded from our analysis.

In addition to computing the predictability of NPP, we also assess the relative importance of the drivers of phytoplankton productivity using the light, nutrient, and temperature limitation terms for the diatom functional group, the group that accounts for the vast majority of total NPP in the Arctic Ocean (Long et al., 2021). The model formulations of these limitation terms are listed in Section S1. We use the N limitation term for diatoms to approximate the role of nutrients in limiting phytoplankton growth. On an annual, pan-Arctic scale, CESM2-LE average N limitation terms are lower (and thus more limiting) than for any other nutrient (Long et al., 2021). Si has a slightly lower limitation term in September on a pan-Arctic basis, but Si availability largely controls phytoplankton functional type dominance in the Arctic, not NPP (Ardyna et al., 2020; Long et al., 2021). To determine the relative limitation (R) for the light (L), N (N), and temperature (T) drivers, we use the modeled limitation terms for light (Lim_L), nitrogen (Lim_N), and temperature (Lim_T), such that:

$$R_{(L,N,T)} = \frac{1 - Lim_{(L,N,T)}}{(1 - Lim_L) + (1 - Lim_N) + (1 - Lim_T)}, \quad (2)$$

where $Lim_{(L,N,T)}$ represents the limitation term for the desired driver. With this formulation (Oliver et al., 2023), limitation proportions for light, temperature, and the most limiting nutrient sum to 1 ($R_L + R_N + R_T = 1$), and the larger the value of the limitation proportion, the more important that driver is in controlling phytoplankton growth. However, both the relative limitation by any driver and the predictability of that limitation term play a role in how important a given driver is in controlling the predictability of NPP. The relative PPP of each limitation term (R_{PPP}), and thus its relative importance in controlling the PPP of NPP, is quantified as

$$R_{PPP} = \frac{R_{(L,N,T)} * PPP_{(L,N,T)}}{(R_L * PPP_L) + (R_N * PPP_N) + (R_T * PPP_T)}, \quad (3)$$

where R represents the relative limitation (calculated in Equation 2) and $PPP_{(L,N,T)}$ represents the PPP of the limitation term (calculated in Equation 1).

To evaluate differences between 2010–2012 and 2030–2032, we use paired t tests (using $\alpha = 0.05$). All statistical analyses are conducted in Python version 3.10.12.

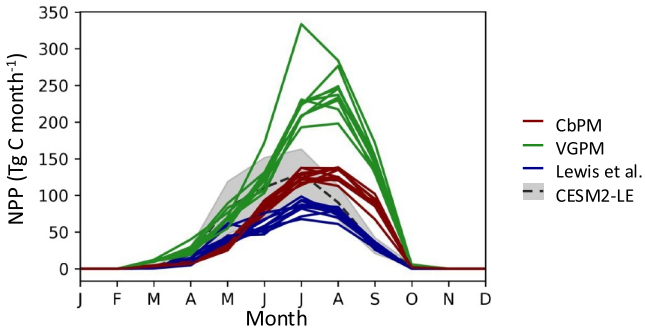

Figure 3. Monthly net primary production (NPP; Tg C per month) for the Arctic Ocean north of 66.5°N from 2005 to 2014 for three satellite algorithms (Behrenfeld & Falkowski, 1997; Lewis et al., 2020; Westberry et al., 2008) and the 2005–2014 mean (black dashed line) and standard deviation (gray area) of 50 ensemble members of the Community Earth System Model version 2 Large Ensemble (CESM2-LE).

3. Results

3.1. Evaluation of Modeled Net Primary Production

CESM2 is a fully coupled Earth system model; each simulation differs due to internal climate variability and represents an equally possible realization of any given variable. In contrast, the observational record is analogous to one iteration of an Earth system model. Therefore, individual years of satellite observations cannot be directly compared to climate model output due to differences in the internal variability of the Earth system. To better understand how observations fit within the range of modeled NPP, we compare modeled 2005–2014 NPP (integrated over the top 100 m, mean of 50 ensemble members) to remote sensing observations using an Arctic-specific NPP algorithm and two global algorithms, VPGM and CbPM. Satellite observations in the Arctic are limited by low sun angle and by sea ice and cloud cover and the unique optical properties of the region mean that satellite estimates are particularly uncertain, with satellite-derived estimates ranging from 200 to 1,000 Tg C yr^{-1} across the region (Babin et al., 2015). For the region >66.5° N, both sea ice cover and the polar night limit light availability, and consequently there is little NPP from October until March. NPP in the CESM2-LE increases from April until July, when phytoplankton produce an average of 130 Tg C per month (Figure 3), and NPP rapidly diminishes again in August and September. Estimates of NPP derived from ocean color using an Arctic-specific algorithm similarly find that NPP peaks in July in almost all years (with the exception of 2010, when NPP peaked in August), with rates of NPP peaking at 67–99 Tg C per month (Figure 3). For both the CbPM and VGPM algorithms, Arctic NPP peaked more frequently in August (in six and 8 years of the 10 spanning from 2005 to 2014, respectively) than in July, and peak NPP averaged 132 and 248 Tg C per month with these two algorithms (Figure 3). On a pan-Arctic scale, the CESM2-LE appears to over-estimate NPP in the spring (Figure 3), but the large under-ice phytoplankton blooms that may be generated across much of the Arctic likely result in substantial underestimates of NPP by satellite observations during this period (Arrigo et al., 2014; Payne et al., 2024). In the fall, NPP in the CESM2-LE is low compared to the global algorithms and slightly higher than the Arctic-specific algorithm (Figure 3), with this spread across satellite algorithms likely attributable to the unique optical properties of the Arctic (Babin et al., 2015; Lewis & Arrigo, 2020). For the 50 members of the CESM2-LE used as a part of this analysis, annually integrated NPP in this region averaged 474 ± 158 Tg C yr^{-1} from 2005 to 2014, while the three satellite algorithms produced average NPP of 306 ± 21, 475 ± 27, and 852 ± 87 Tg C yr^{-1} for the Lewis et al. (2020), CbPM (Westberry et al., 2008), and VGPM algorithms (Behrenfeld & Falkowski, 1997), respectively (Figure 3).

Spatially across the Arctic Ocean and sub-Arctic seas (>50°N), the CESM2-LE replicates broad patterns of annual NPP but produces too little NPP in coastal regions (Figure 4). The model produces lower NPP in the central Arctic and extending down the east coast of Greenland and as far south as Hudson Bay, while higher annual NPP is observed in the north Atlantic and in the Bering and Barents Seas (Figure 4a). The two global algorithms have similar spatial patterns of high and low NPP, with perhaps the biggest discrepancy in Hudson Bay, where VGPM and CbPM both observe more NPP than the CESM2-LE produces (Figure 4). Elevated NPP between Iceland, Svalbard, and Norway is observed in the model and across all three satellite algorithms (Figure 4). While both CbPM and VGPM produce very high NPP close to the coast in Alaska and Scandinavia (Figures 4c and 4d), the CESM2-LE looks more comparable to the Lewis et al. (2020) algorithm (Figures 4a and 4b), likely because the global algorithms overestimate Chlorophyll-*a* concentrations in these waters, leading to an overestimate of NPP. Overall, this evaluation indicates that CESM2-LE adequately reproduces the seasonal cycle of NPP in the Arctic observed across different satellite algorithms, as well as broad spatial patterns of annual NPP produced remotely.

3.2. Predictability of Net Primary Production in 2010 and 2030

On a pan-Arctic (>50°N) scale, modeled phytoplankton NPP peaks in May, with nearly 25% of total annual NPP generated in the month of May (greyscale gradients in background of Figure 5). June and July are similarly highly productive and account for 22% and 16% of total NPP, respectively. April, August, and September contribute

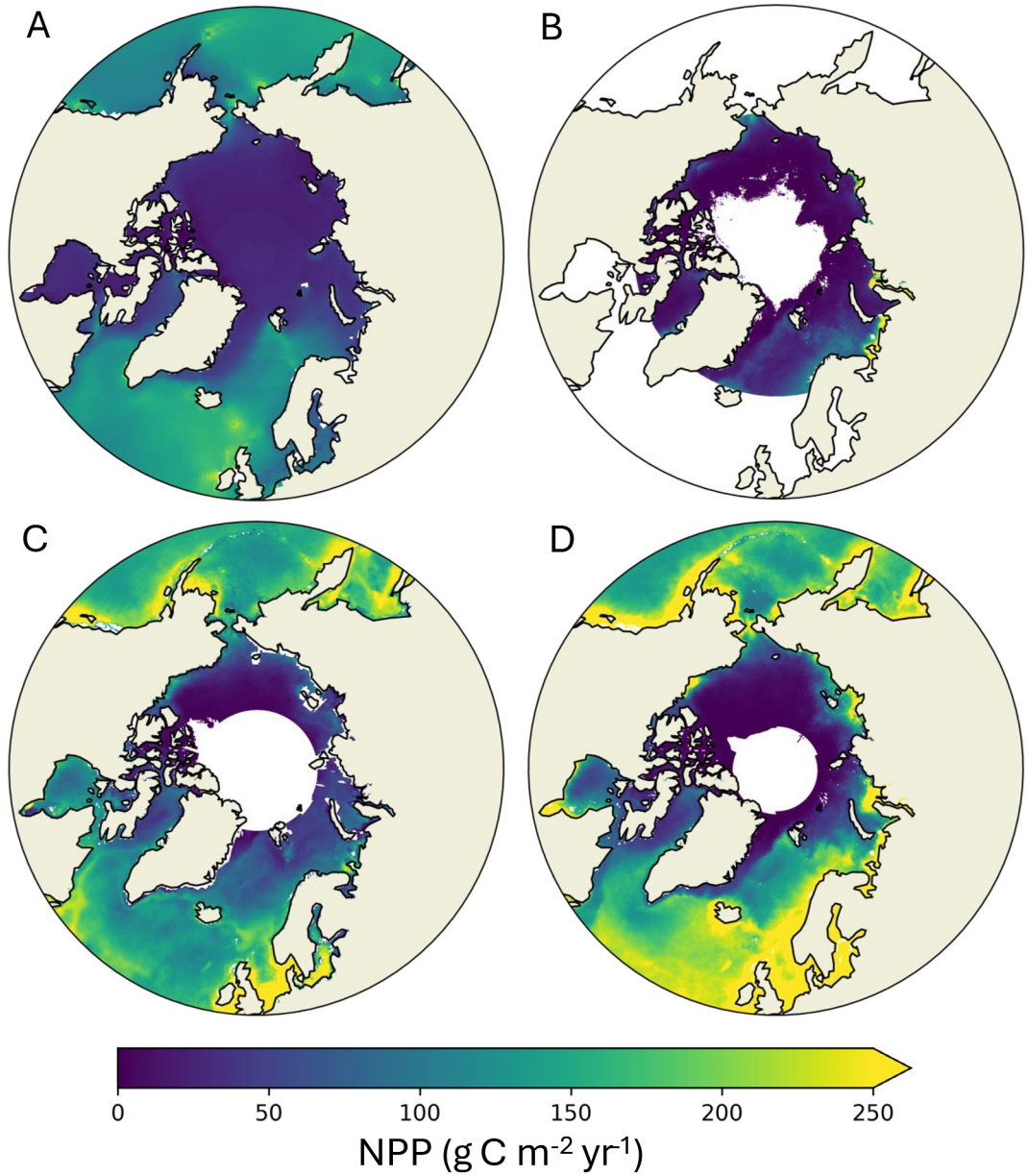

Figure 4. Mean annual integrated net primary production (NPP; g C m^{-2} yr^{-1}) for the Arctic Ocean north of 50°N from (a) the CESM2-LE and satellite-derived NPP produced by (b) an Arctic-specific algorithm (Lewis & Arrigo, 2020), (c) the VPGM (Behrenfeld & Falkowski, 1997), and (d) the CbBM (Westberry et al., 2008) for 2005–2014.

12%, 12% and 6%, respectively, to annual NPP, while the months of October-March generate a total of 8% of annual NPP. Consequently, we focus our analysis on changes to predictability from May–July.

For both the 2010 and 2030 sets of perfect model forecasts, the PPP for NPP is high (>0.75) in the initialization month (Figure 5) due to low initial variance among the perfect model experiments (i.e., small spread across the forecast ensemble). However, in the first month after initialization, PPP drops substantially, with PPP gradually increasing across most initializations during the subsequent summer and fall months (May–November) and sharply falling off in the winter (December-February) months. While there are some differences in monthly PPP across the different initialization months, PPP generally follows the same temporal evolution across all initialization months, indicating that Arctic NPP predictability is relatively insensitive to the forecast initialization month (Table 1, Figure 5).

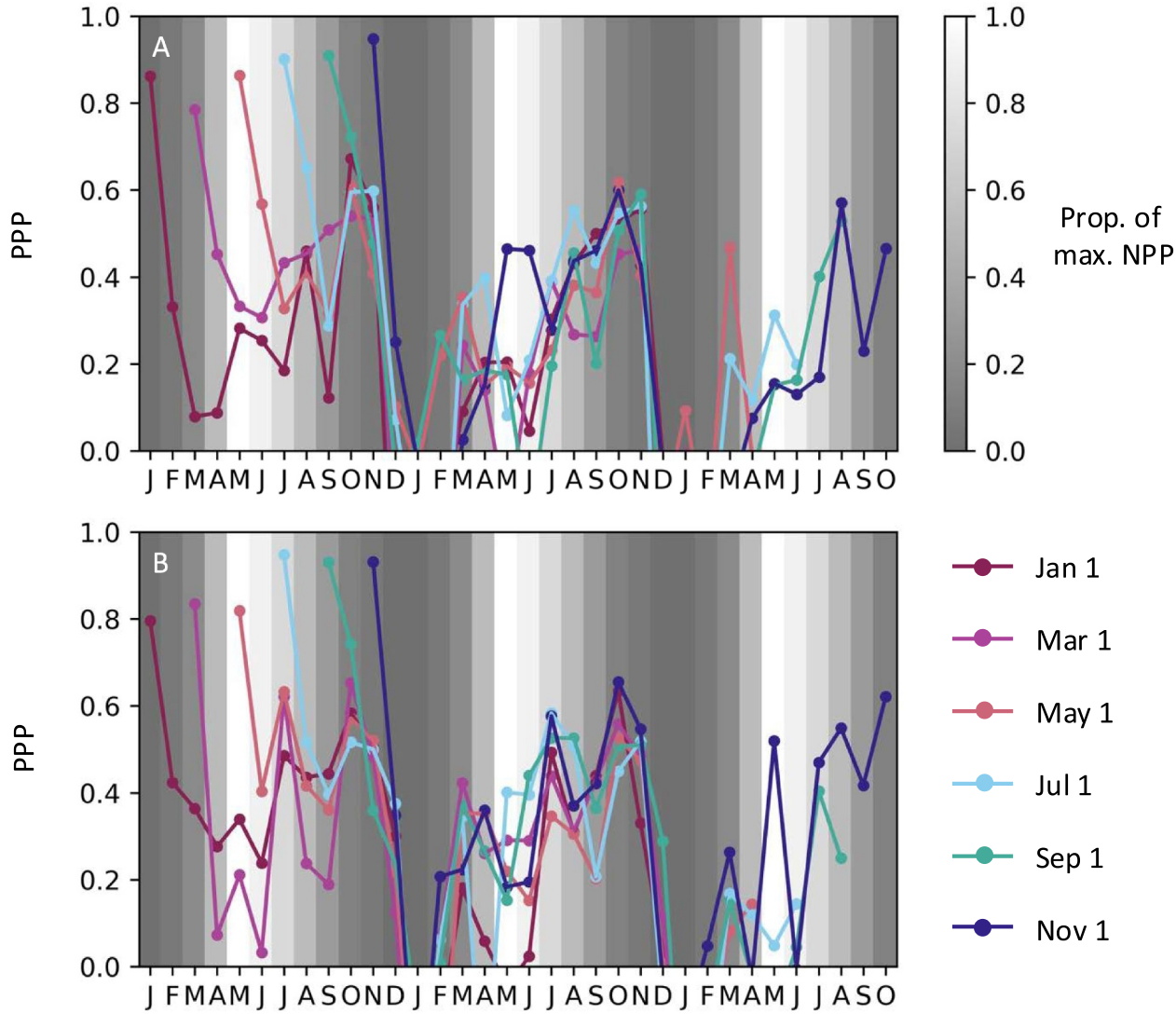

Figure 5. Monthly Prognostic Potential Predictability (PPP) of net primary production (NPP) for (a) January 2010–October 2012 and (b) January 2030–October 2032 for the Arctic Ocean (> 50°N). Line colors indicate when simulations were initialized (1 January, 1 March, 1 May, 1 July, 1 September1 , and 1 November), and background gradient indicates the proportion of the maximum NPP generated in each month. *Y*-axis limits are set to exclude negative PPP values where there is no predictive skill.

When only the most productive months (May–July) are taken into account, PPP values for forecasts initialized in the 2010s are lower than PPP for forecasts initialized in the 2030s on a pan-Arctic scale. Most individual months demonstrate no change in PPP over this period with the exception of July of 2031, which has a significantly higher PPP (mean of 0.50) than July of 2011 (mean of 0.20, respectively; $p = 0.007$; Figure 5). However, mean PPP values during the most productive months (May–July) across each initialization month are significantly higher in the 2030s than in the 2010s (Table 1). Differences in pan-Arctic PPP between the 2010s and 2030s arise from both a change in climatological variance and forecast ensemble variance. Variance in Arctic NPP in the CESM2-LE is 7.7% greater for 2010–2012 than for 2030–2032 (Table 2). Among the forecast ensembles, variance in 2010–2012 is on average 10.9% greater than in 2030–2032 (Table 2). Forecast ensembles initialized in January and September have far higher variance in the 2010s, while ensembles initialized in May and November have only modestly more variance in the 2010s and ensembles initialized in March and July exhibit more variance in the 2030s (Table 2).

Table 1
Mean May–July Prognostic Potential Predictability (PPP) by Initialization Month for the 2010–2012 and 2030–2032 Periods, Excluding PPP Values Below 0, As Well As the Mean and Standard Deviation (SD) Across Initialization Months and the p-Value of the Paired t Test Comparing 2010–2012 and 2030–2032

Period	Jan	Mar	May	Jul	Sep	Nov	Mean ± SD	*p*-value
2010–2012	0.21	0.33	0.39	0.35	0.22	0.28	0.30 ± 0.07	
2030–2032	0.32	0.31	0.43	0.42	0.31	0.39	0.36 ± 0.05	0.018

Table 2
Change in Variance (Δ,%) in Phytoplankton NPP Across the Arctic Between the 2010s and 2030s for the Climatology and Forecast Ensembles and for Each Initialization Month

	Δ Variance
Climatology	−7.7
Forecast	−10.9
January	−29.1
March	13.3
May	−5.1
July	7.9
September	−39.4
November	−15.3

We investigate regional predictability by separating the Arctic (>66.5°N) from the sub-Arctic (50–66.5°N) and the shelf (<1,000 m) from the deep ocean (>1,000 m) areas, as well as by LME (Table 3). On regional scales, the Arctic shelves stand out as having consistently high productive-season predictability in the 2010s but lowered predictability in the 2030s (Figure 6), while the sub-Arctic shelves and deep ocean also demonstrate relatively high predictability (Table 3; Figures S1–S3). PPP values for the most productive months (May–July) were highest on Arctic shelves in the 2010s (PPP = 0.46; Figure 6a) and were also relatively high in the sub-Arctic shelf (PPP = 0.34; Figure S2a) and sub-Arctic deep ocean (PPP = 0.33, Figure S3a). In the 2030s, however, PPP was highest on the sub-Arctic shelves and deep ocean (PPP = 0.39 for both; Figures S2b and S3b) and was significantly lower on the Arctic shelves than it had been in the 2010s (PPP = 0.37, $p = 0.032$; Figure 6b). During just the most productive month (May in both the sub-Arctic shelves and deep ocean), PPP decreased in the sub-Arctic shelves but increased in the sub-Arctic deep ocean (Table 3; Figures S2 and S3) between 2011 and 2031. On the Arctic shelves, where NPP is equally high in June and July, PPP decreased in June 2031 relative to 2011 and did not change in July 2031 relative to 2011 (Table 3). The Arctic deep ocean had the lowest predictability of any region and did not significantly change between the 2010s and 2030s (Table 3; Figure S1). We also quantified PPP for 20 LMEs in the Arctic, as well as for the Atlantic Ocean (>50°N). The five LMEs with the highest PPP during their most productive month across all initializations and for the 2010s and 2030s are the Canadian East Arctic, East Siberian, Beaufort Sea, Kara Sea, and Laptev Sea LMEs (Table 3), all of which are primarily located on Arctic shelves.

3.3. Which Regions Are Responsible for Increases in Future Predictability?

To investigate which regions drove the pan-Arctic increase in predictability by 2030, we focus on May–July of 2011 and 2031 of a single initialization timing (May 1-initialized). This particular initialization month had pan-Arctic PPP values close to the average across all initialization months (Figure 5) as well as similar spatial patterns of changes between the 2010s and 2030s (compare Figure 7 to Figure S4). Although the increase in predictability in the 2030s is subtle on a pan-Arctic scale, clear regional patterns are visible for the months of May–July, whereby increases in predictability shift northward over the productive summer months. In May, the largest increases in PPP from 2011 to 2031 occured in Hudson Bay, the Iceland LME, and the southern Barents Sea (Figure 7a). May PPP also increases from 2011 to 2031 in the Gulf of Alaska, the Siberian Sea, the Sea of Okhotsk, the northern Norwegian Sea, and the north Atlantic (Figure 7a). In contrast, May PPP declines from 2011 to 2031 in the southern Bering Sea, the northern Chukchi Sea, the central Arctic, the northern Barents Sea, and the Kara Sea (Figure 7a). PPP is most enhanced in June 2031 relative to June 2011 in the shelf regions of the Arctic—in Baffin Bay and the Beaufort, Chukchi, Siberian, Laptev, Kara, and northern Barents Seas—as well as in the eastern Bering Sea (Figure 7b). PPP exhibits slight increases from 2011 to 2031 across the Arctic, with Hudson Bay, the Sea of Okhotsk, and the southern North Atlantic all showing moderate increases in 2031 June PPP relative to 2011 (Figure 7b). June PPP declines from 2011 to 2031 in the central Arctic and the Norwegian Sea (Figure 7b). PPP in July 2031 exhibits large increases relative to PPP in July 2011 in the central Arctic, with July PPP increases also apparent in the north Atlantic, the Siberian, Laptev, and Kara Seas, and the northern Gulf of Alaska (Figure 7c). In contrast, July PPP shows moderate declines in 2031 relative to 2011 in coastal areas throughout the Arctic, including in the Sea of Okhotsk, the Norwegian Sea, Baffin Bay, and parts of the coastal Barents Sea (Figure 7c).

3.4. What Drives Predictability?

NPP is controlled by temperature and the availability of light and nutrients. We quantified the importance of these drivers in controlling the predictability of NPP on a pan-Arctic basis as well as by LME and by region. However, the primary drivers were not significantly different between LMEs or by region, and consequently we present only our results on a pan-Arctic basis here.

Between October and April, when much of the Arctic is covered with sea ice, the light limitation is the most important of these factors, accounting for ∼50% of the total limitation on pan-Arctic phytoplankton growth

Table 3
Net Primary Production (NPP; g C m^{-2} d^{-1}) and Mean Prognostic Potential Predictability (PPP) Across All Initialization Timings Forecasts for 2011 ('11) and 2031 ('31) for May, June, and July for Each of the 20 Large Marine Ecosystems (LMEs) and for the North Atlantic (>50°N)

LME	Region	May NPP	May '11 PPP	May '31 PPP	June NPP	June '11 PPP	June '31 PPP	July NPP	July '11 PPP	July '31 PPP
	Arctic shelf	0.21	0.35	0.20	**0.33**	**0.45**	**0.10**	**0.33**	**0.51**	**0.48**
N. Bering and Chukchi Seas	Arctic shelf	0.45	0.12	0.21	**0.51**	**0.05**	**0.15**	0.43	0.36	0.23
Beaufort Sea	Arctic shelf	0.05	–	0.05	0.23	0.24	0.15	**0.28**	**0.75**	**0.63**
E. Siberian Sea	Arctic shelf	0.03	–	–	0.18	–	0.05	**0.26**	**0.75**	**0.79**
Laptev Sea	Arctic shelf	0.04	–	0.11	0.15	–	0.02	**0.24**	**0.52**	**0.65**
Canadian High Arctic	Arctic shelf	0.01	0.52	0.68	0.06	–	0.71	**0.18**	**0.12**	**0.54**
Kara Sea	Arctic shelf	0.08	0.24	0.14	0.28	0.39	0.39	**0.34**	**0.64**	**0.60**
Canadian E. Arctic	Arctic shelf	0.37	0.80	0.47	**0.57**	**0.91**	**0.41**	0.49	0.73	0.44
Barents Sea	Arctic shelf	0.49	0.48	0.36	**0.51**	**0.34**	**0.13**	0.39	0.32	0.11
	Arctic deep	0.22	0.32	0.19	0.24	–	–	**0.33**	**0.31**	**0.32**
Central Arctic	Arctic deep	0.00	0.15	–	0.06	0.21	–	**0.30**	–	**0.44**
Greenland Sea	Arctic deep	0.51	0.59	0.48	**0.54**	**0.28**	**0.27**	0.42	0.24	-
Norwegian Sea	Arctic deep	**1.39**	**0.14**	**0.27**	0.97	0.18	0.23	0.51	0.27	0.12
	Sub-Arctic shelf	**0.89**	**0.26**	**0.15**	0.73	0.23	0.34	0.50	0.31	0.46
Sea of Okhotsk	Sub-Arctic shelf	**1.31**	**0.29**	**0.26**	1.00	0.20	0.26	0.56	0.18	0.17
Hudson Bay	Sub-Arctic shelf	0.12	–	–	0.30	0.54	0.69	**0.30**	**0.87**	**0.83**
Newfoundland-Labrador	Sub-Arctic shelf	**0.94**	**0.44**	**0.41**	0.61	0.40	0.43	0.45	0.62	0.29
Iceland Sea and Shelf	Sub-Arctic shelf	**1.19**	**0.38**	**0.50**	0.98	0.26	0.19	0.57	0.27	0.19
North Sea	Sub-Arctic shelf	**0.83**	**0.22**	**0.15**	0.61	0.06	0.35	0.49	0.17	0.21
	Sub-Arctic deep	**1.2**	**0.11**	**0.31**	0.97	0.09	0.29	0.57	0.39	0.5
Gulf of Alaska	Sub-Arctic deep	**0.68**	**0.26**	**0.50**	0.49	0.24	0.08	0.41	0.12	0.05
W. Bering Sea	Sub-Arctic deep	**1.28**	**0.28**	**0.09**	1.16	0.18	0.21	0.59	0.27	0.09
Aleutian Islands	Sub-Arctic deep	1.06	0.24	0.15	**1.25**	**0.13**	**0.30**	0.81	0.21	0.18
E. Bering Sea	Sub-Arctic deep	**1.08**	**0.25**	**0.26**	0.95	0.21	0.37	0.57	0.28	0.31
North Atlantic	Sub-Arctic deep	**1.33**	**0.12**	**0.41**	1.04	0.18	0.22	0.61	0.19	0.42

Note. PPP Values Below 0 are Excluded From Means. LMEs are organized by the dominant region (sub-Arctic or Arctic and deep ocean or shelf), and mean NPP and PPP values for each region are also presented. Bold indicates the month(s) with the highest NPP for each LME.

(Figure 8a). However, light limitation drops in importance between May and July (dipping to a minimum of 34% in July) as sea ice retreats before increasing again in the fall as day length declines. Temperature limitation is far more consistent, accounting for 45%–47% of the total phytoplankton growth limitation throughout the year, and thus is the dominant limitation term during the summer months (May–August) when NPP is greatest (Figure 8a). Finally, N limitation (which we use here to approximate the overall role of nutrients in limiting growth—see

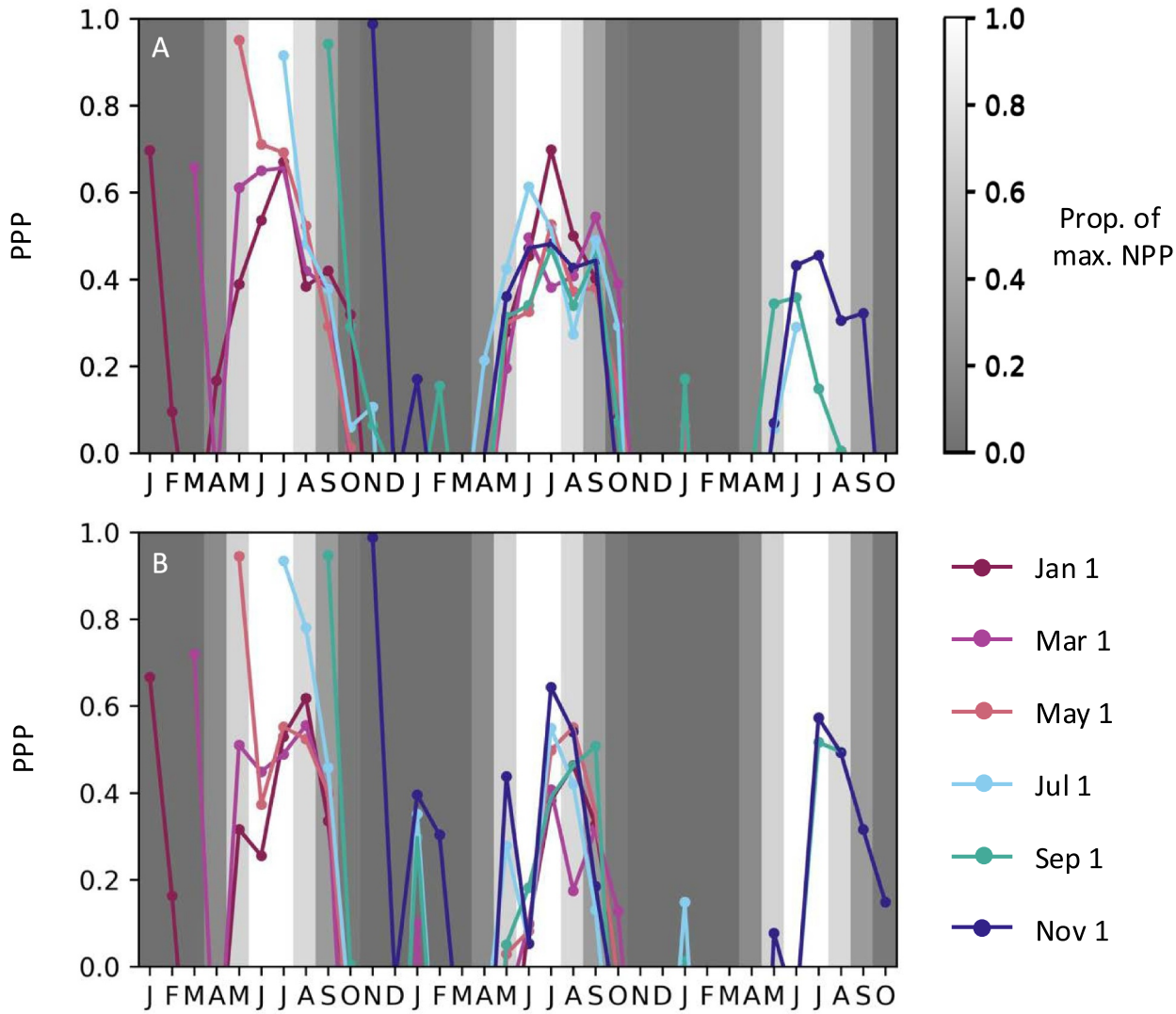

Figure 6. Monthly Prognostic Potential Predictability (PPP) of net primary production (NPP) for (a) January 2010–October 2012 and (b) January 2030–October 2032 for the Arctic shelves (> 66.5°N; <1,000 m). Line colors indicate when simulations were initialized (1 January, 1 March, 1 May, 1 July, 1 September, and 1 November), and background gradient indicates the proportion of the maximum NPP generated in each month. Y-axis limits are set to exclude negative PPP values where there is no predictive skill.

Section 2.3) remains <6% between October and April and increases as NPP increases over the summer months, peaking in July, when it accounts for 19% of the total limitation of phytoplankton growth (Figure 8a).

Light, temperature, and N control the predictability of NPP not only through their relative importance as limitations, but also through their predictability. While light limitation is initially predictable (PPP of 0.81–0.94 during the initialization month of May; Figure 8b), its predictability rapidly declines. The PPP of light limitation increases again in the summer months of the first year of the simulations (July–October), but declines substantially by the second year (Figure 8b). The PPP of temperature limitation also declines following initialization, reaching a low in the summer or autumn of the first year of the simulations (Figure 8b), but recovers and remains elevated in the second year of the simulations, remaining above the significance line throughout the 2-year forecasts (Figure 8b). Finally, N limitation declines more slowly than light limitation, increases during the winter of the first year, and declines in the summer of the second year of the forecasts (Figure 8b).

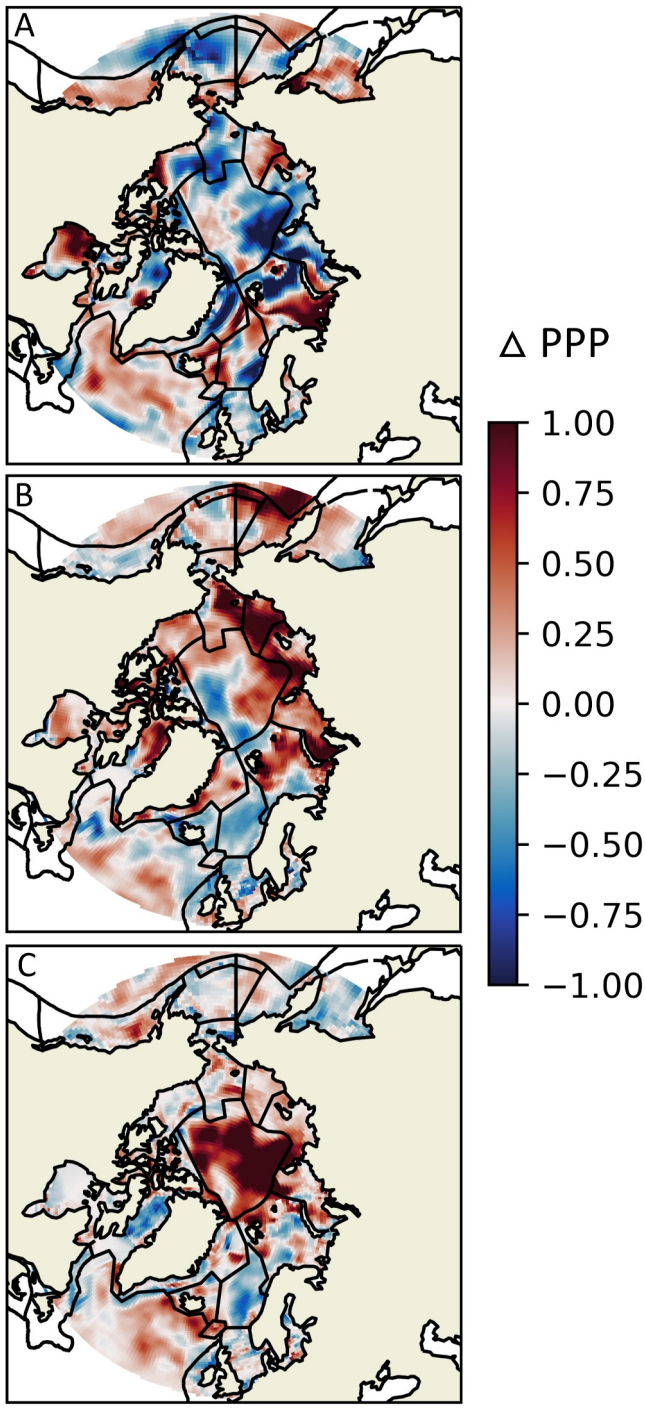

Figure 7. Δ PPP for (a) May 2031– May 2011, (b) June 2031 – June 2011, and (c) July 2031 – July 2011 for simulations initialized on 1 May 2030 and 2010. Black lines indicate large marine ecosystem (LME) boundaries.

To determine which of these limitation terms most controls the predictability of NPP, we combine the relative importance and PPP of each limitation term (see Equation 3) and calculate its relative PPP. While temperature initially has a relative PPP of 0.52, its contribution to PPP rises in importance during the late summer and autumn, peaking at 0.91 by January (Figure 8c). The relative PPP of temperature declines once again in the spring of the second year but rebounds by the autumn of the second year. While light starts off as a similarly important contributor to PPP as temperature, with a relative PPP of 0.41, it declines through the summer and autumn and is only intermittently contributing to the predictability of NPP by the second year (Figure 8c). N limitation is variable in its initial importance depending on initialization month, with a relative PPP of 0.07 for May-initialized forecasts. The relative PPP of N limitation never rises above 0.18 and it contributes the most to the predictability of NPP in July (Figure 8c), the month when its relative limitation is greatest. Overall, this demonstrates that, because of its importance as a limit on phytoplankton growth and because of its high predictability, temperature limitation is the most important driver in controlling the predictability of phytoplankton NPP across the Arctic in both 2010 and 2030 (see Figure S5).

4. Discussion

Here, we use 2-year perfect model forecasts to quantify the potential upper limit of predictability of NPP in the Arctic Ocean and sub-Arctic seas in the 2010s and 2030s. We find that Arctic NPP is predictable for at least 2 years during the months with the most phytoplankton production, and that predictability may moderately increase in 2030 relative to 2010. Further, we find that the Arctic shelves provide much of this predictability. Finally, we identify temperature as the primary driver of the predictability of NPP, due both to its importance as a limit on phytoplankton growth during the summer months and because of its high interannual predictability.

Phytoplankton NPP in the Arctic Ocean is highly seasonal and experiences substantial interannual variability, but our results indicate that operational forecasts may provide moderately skillful predictions of Arctic NPP for multiple years. This predictability is greatest on the shallow continental shelves of the Arctic Ocean, where most small-scale, indigenous-operated Arctic fisheries are currently located (Tai et al., 2019) and where fisheries are projected to expand substantially in the future (Christiansen et al., 2014). Both the sub-Arctic shelves and sub-Arctic deep ocean also show a relatively high degree of predictability, indicating that forecasts of NPP may even prove useful in regions with some of the world's largest present-day fisheries (Christiansen et al., 2014; Hollowed & Sundby, 2014). A number of other recent studies have evaluated the predictability of phytoplankton NPP globally (Krumhardt et al., 2020; A. Xu et al., 2023; Yeager et al., 2022) as well as in polar regions (Buchovecky et al., 2023; Fransner et al., 2023), often finding that predictions of NPP are skillful. Interestingly, NPP has often proven more predictable than the drivers of phytoplankton production. For example, work by Séférian et al. (2014) in the tropical Pacific finds that, despite substantial interannual variability, NPP is more predictable than temperature, the primary driver of that variability. Forecasts of the spring bloom along the sea ice edge of the Southern Ocean are skillful 7–10 years in advance (Buchovecky et al., 2023), while sea ice extent in the Southern Ocean is only predictable 11 months in advance (Bushuk et al., 2021). Similarly, we find that the predictability of NPP persists over the 2 years of our forecast ensembles, even though the predictability of sea ice, which acts as a key control on Arctic

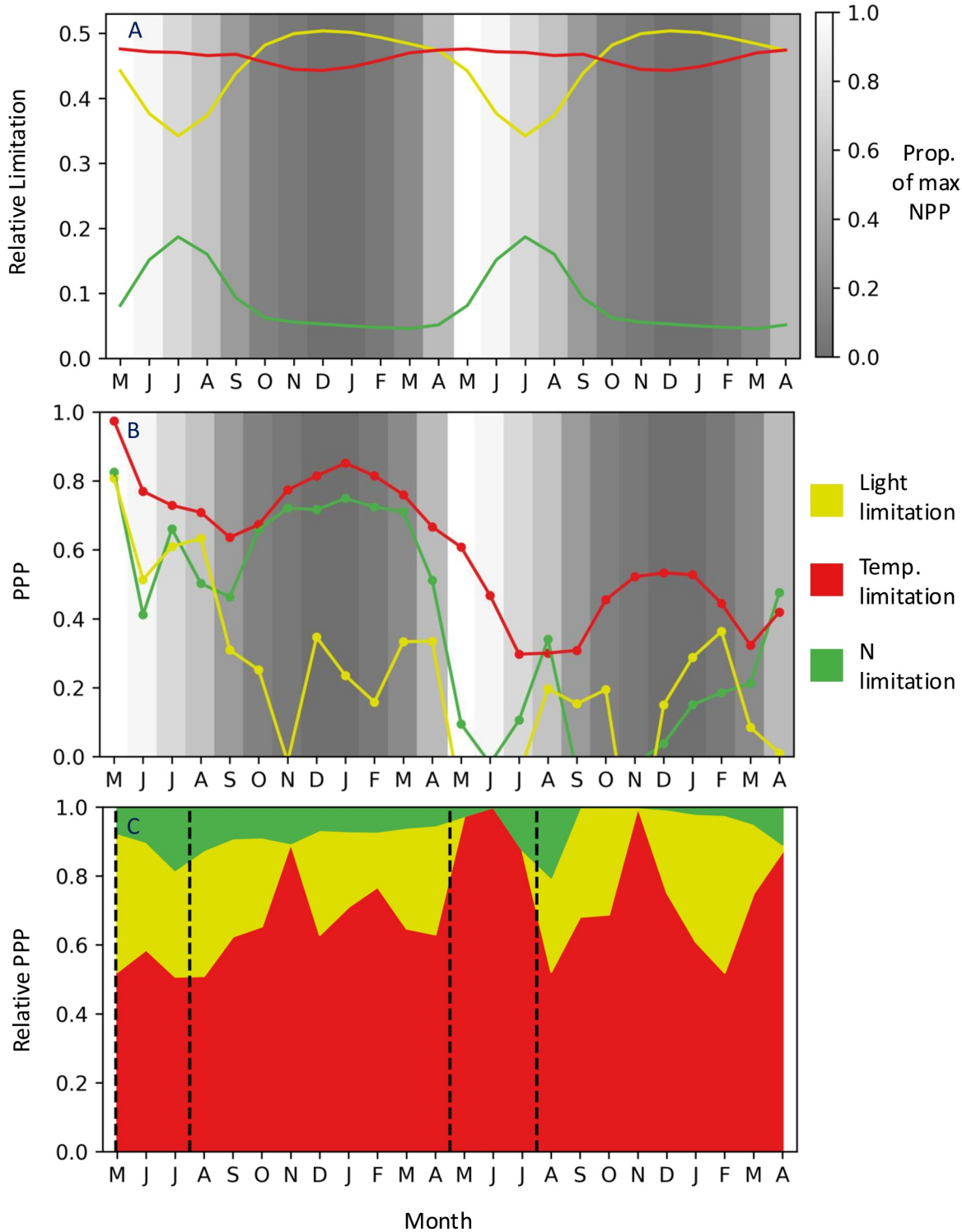

Figure 8. (a) The climatological monthly proportional importance of light (yellow), temperature (red), and nitrogen (green) limitation terms in controlling NPP across the Arctic in the CESM2-LE for 2010–2012. Background gradient indicates the proportion of maximum climatological NPP reached during each month. (b) Monthly Prognostic Potential Predictability (PPP) for light (yellow), temperature (red), and nitrogen (green) limitation terms on a pan-Arctic scale for simulations initialized on 1 May 2010 and concluding 30 April 2012. Background gradient indicates the proportion of maximum NPP reached during each month. Horizontal dashed line indicates line of statistical significance. (c) The importance of N (green), light (yellow), and temperature (red) limitation terms in controlling the PPP of NPP across the Arctic. Dashed lines demarcate the May–July period with the highest NPP.

phytoplankton by affecting both light availability and upper ocean temperatures (Blanchard-Wrigglesworth, Armour, et al., 2011), declines substantially as lead time increases (Holland & Hunke, 2022).

We also investigate how predictability changes as the Arctic climate system evolves and find that NPP is significantly more predictable during the most productive months in the 2030s than in the 2010s, thus indicating that the skill of forecasts for Arctic NPP may increase in the near future. This increase in predictability for NPP stands in contrast to the predictability of sea ice extent in the first several decades of the 21st century. Prior work using perfect model experiments initialized from the CESM1-LE finds that summer Arctic sea ice reached peak predictability in 2010, with lower predictability in both 2000 and in 2021 (Holland et al., 2019). This increase and subsequent decline in predictability is associated with a large increase in the internal variability of sea ice from 2000 to 2030 and a slower increase in forecast variability over this same period (Holland et al., 2019), resulting in a window of enhanced sea ice extent prediction and possibly explaining the decline we find in the predictability of NPP on the Arctic shelves in some months of the 2030s relative to the 2010s. Similarly, the climate-driven change in Arctic NPP predictability arises from changes to both climatological and forecast variance. Between 2010 and 2030, the climatological variance declines by almost 8% while the variance between forecast ensembles declines by nearly 11%, indicating that both a reduction in the internal variability of Arctic NPP and increased forecast skill may play a role in driving improvements in predictions of NPP.

Finally, our results indicate that the primary driver of predictability for Arctic NPP is ocean temperatures, which both act as the most important limit on phytoplankton growth during the summer months and remain highly predictable over our 2-year forecasts. Although massive phytoplankton blooms have been observed under sea ice and at very low temperatures (Arrigo et al., 2014), both laboratory studies (Coello-Camba & Agustí, 2017) and modeling studies that use different methodologies (Krumhardt et al., 2020) suggest that Arctic Ocean temperatures substantially limit phytoplankton growth. In a previous global study of the potential predictability of NPP, high-latitude environments where temperatures and light are the most important limitations on phytoplankton growth have far lower potential predictability than areas primarily controlled by nutrient limitation (Krumhardt et al., 2020). However, ocean temperatures have also been shown to be key in providing predictability to sea ice extent (Bushuk et al., 2017) as well as to NPP (L. Xu et al., 2023).

While our results suggest that CESM2 and other ESMs may provide moderately skillful predictions of NPP in the Arctic, challenges remain in implementing actionable forecasts of regional NPP. Perfect model forecasts such as those used in this study do not require a skillful model, instead providing an upper limit of predictability for a variable that models may not yet capture accurately (Holland et al., 2019; Krumhardt et al., 2020). Here, we demonstrate that the CESM2-LE reasonably replicates both the seasonality and total annual phytoplankton NPP produced by Arctic-tuned satellite algorithms. However, remotely sensed NPP has many limitations in the Arctic. Satellites cannot provide direct estimates of large under-ice phytoplankton blooms (Arrigo et al., 2012; Payne et al., 2024), leading to estimates of annual NPP an order of magnitude lower than observations (Arrigo et al., 2014). Further, satellite-derived estimates of NPP may underestimate NPP generated in the subsurface or in the fall, when sun angle prevents satellite observations (Babin et al., 2015; Brown et al., 2015; Lee et al., 2015). While CESM2 and other ESMs may still have lower skill at predicting in situ NPP, our results demonstrate that these models can forecast phytoplankton NPP reasonably well for at least 2 years, which may help in future marine resource management.

Data Availability Statement

The CESM2 Large Ensemble (Danabasoglu et al., 2023) is available at: https://www.earthsystemgrid.org/dataset/ucar.cgd.cesm2le.output.html. The perfect model prediction forecasts (Holland & Bailey, 2024a, 2024b) are available at https://rda.ucar.edu/datasets/ds651.1 for 2010 and https://rda.ucar.edu/datasets/ds651.3 for 2030. Remotely sensed NPP files are available at http://orca.science.oregonstate.edu/1080.by.2160.monthly.hdf.cbpm2.m.php for the Carbon-based Production Model (Westberry et al., 2008), http://orca.science.oregonstate.edu/1080.by.2160.monthly.hdf.vgpm.m.chl.m.sst.php for the Vertically Generalized Production Model (Behrenfeld & Falkowski, 1997), and http://albedo.stanford.edu/gertvd/research/arctic/prod/prod_data/Reg/ for the Arctic-specific algorithm (Lewis & Arrigo, 2020). Scripts used to create all figures presented in this article can be found at https://github.com/courtneympayne93/ArcticPerfectPrediction. Shapefiles for Large Marine Ecosystems can be found at https://www.sciencebase.gov/catalog/item/55c77722e4b08400b1fd8244.

Acknowledgments
CMP and NSL are grateful for support from the National Science Foundation (OCE-1752724). AKD, MMH, and KMK are grateful for support from National Science Foundation (Award 2103843). This work uses resources supported by the U.S. National Science Foundation National Center for Atmospheric Research (NSF NCAR) under cooperative agreement 1852977. Computing and data storage resources were provided by the Computational and Information Systems Laboratory (CISL) at NSF NCAR. We thank all the scientists, software engineers, and administrators who contributed to the development of CESM2.

References

Ardyna, M., Babin, M., Gosselin, M., Devred, E., Rainville, L., & Tremblay, J.-É. (2014). Recent Arctic Ocean sea ice loss triggers novel fall phytoplankton blooms. *Geophysical Research Letters*, *41*(17), 6207–6212. https://doi.org/10.1002/2014GL061047

Ardyna, M., Mundy, C. J., Mills, M. M., Oziel, L., Grondin, P.-L., Lacour, L., et al. (2020). Environmental drivers of under-ice phytoplankton bloom dynamics in the Arctic Ocean. *Elementa: Science of the Anthropocene*, *8*, 30. https://doi.org/10.1525/elementa.430

Arrigo, K. R., Perovich, D. K., Pickart, R. S., Brown, Z. W., Van Dijken, G. L., Lowry, K. E., et al. (2012). Massive phytoplankton blooms under Arctic sea ice. *Science*, *336*(6087), 1408. https://doi.org/10.1126/science.1215065

Arrigo, K. R., Perovich, D. K., Pickart, R. S., Brown, Z. W., Van Dijken, G. L., Lowry, K. E., et al. (2014). Phytoplankton blooms beneath the sea ice in the Chukchi sea. *Deep-Sea Research Part II Topical Studies in Oceanography*, *105*, 1–16. https://doi.org/10.1016/j.dsr2.2014.03.018

Arrigo, K. R., & Van Dijken, G. L. (2011). Secular trends in Arctic Ocean net primary production. *Journal of Geophysical Research*, *116*(9), 1–15. https://doi.org/10.1029/2011JC007151

Arrigo, K. R., & Van Dijken, G. L. (2015). Continued increases in Arctic Ocean primary production. *Progress in Oceanography*, *136*, 60–70. https://doi.org/10.1016/j.pocean.2015.05.002

Ashjian, C. J., Campbell, R. G., Welch, H. E., Butler, M., & Van Keuren, D. (2003). Annual cycle in abundance, distribution, and size in relation to hydrography of important copepod species in the western Arctic Ocean. *Deep-Sea Research Part I Oceanographic Research Papers*, *50*(10–11), 1235–1261. https://doi.org/10.1016/S0967-0637(03)00129-8

Babin, M., Bélanger, S., Ellingsen, I., Forest, A., Le Fouest, V., Lacour, T., et al. (2015). Estimation of primary production in the Arctic Ocean using ocean colour remote sensing and coupled physical–biological models: Strengths, limitations and how they compare. *Progress in Oceanography*, *139*, 197–220. https://doi.org/10.1016/j.pocean.2015.08.008

Beer, E., Eisenman, I., & Wagner, T. J. W. (2020). Polar amplification due to enhanced heat flux across the Halocline. *Geophysical Research Letters*, *47*(4). https://doi.org/10.1029/2019GL086706

Behrenfeld, M. J., & Falkowski, P. G. (1997). Photosynthetic rates derived from satellite-based chlorophyll concentration. *Limnology & Oceanography*, *42*(1), 1–20. https://doi.org/10.4319/lo.1997.42.1.0001

Blanchard-Wrigglesworth, E., Armour, K. C., Bitz, C. M., & DeWeaver, E. (2011a). Persistence and inherent predictability of Arctic sea ice in a GCM ensemble and observations. *Journal of Climate*, *24*(1), 231–250. https://doi.org/10.1175/2010JCLI3775.1

Blanchard-Wrigglesworth, E., Bitz, C. M., & Holland, M. M. (2011b). Influence of initial conditions and climate forcing on predicting Arctic sea ice: Arctic sea ice predictability. *Geophysical Research Letters*, *38*(18). https://doi.org/10.1029/2011GL048807

Blanchard-Wrigglesworth, E., & Bushuk, M. (2019). Robustness of Arctic sea-ice predictability in GCMs. *Climate Dynamics*, *52*(9–10), 5555–5566. https://doi.org/10.1007/s00382-018-4461-3

Boertmann, D., Lyngs, P., Merkel, F. R., & Mosbech, A. (2004). The significance of Southwest Greenland as winter quarters for seabirds. *Bird Conservation International*, *14*(2), 87–112. https://doi.org/10.1017/S0959270904000127

Bradstreet, M. S., & Cross, W. E. (1982). Trophic relationships at high arctic ice edges. *Arctic*, *35*(1), 1–12. https://doi.org/10.14430/arctic2303

Brodie, S., Pozo Buil, M., Welch, H., Bograd, S. J., Hazen, E. L., Santora, J. A., et al. (2023). Ecological forecasts for marine resource management during climate extremes. *Nature Communications*, *14*(1), 7701. https://doi.org/10.1038/s41467-023-43188-0

Brown, Z. W., Lowry, K. E., Palmer, M. A., Van Dijken, G. L., Mills, M. M., Pickart, R. S., & Arrigo, K. R. (2015). Characterizing the subsurface chlorophyll a maximum in the Chukchi Sea and Canada basin. *Deep-Sea Research Part II Topical Studies in Oceanography*, *118*, 88–104. https://doi.org/10.1016/j.dsr2.2015.02.010

Buchovecky, B., MacGilchrist, G. A., Bushuk, M., Haumann, F. A., Frölicher, T. L., Le Grix, N., & Dunne, J. (2023). Potential predictability of the spring bloom in the Southern Ocean sea ice zone. *Geophysical Research Letters*, *50*(20), e2023GL105139. https://doi.org/10.1029/2023GL105139

Bushuk, M., Msadek, R., Winton, M., Vecchi, G. A., Gudgel, R., Rosati, A., & Yang, X. (2017). Skillful regional prediction of Arctic sea ice on seasonal timescales. *Geophysical Research Letters*, *44*(10), 4953–4964. https://doi.org/10.1002/2017GL073155

Bushuk, M., Winton, M., Haumann, F. A., Delworth, T., Lu, F., Zhang, Y., et al. (2021). Seasonal prediction and predictability of regional antarctic sea ice. *Journal of Climate*, *34*(15), 6207–6233. https://doi.org/10.1175/JCLI-D-20-0965.1

Campbell, J. W. (1995). The lognormal distribution as a model for bio-optical variability in the sea. *Journal of Geophysical Research*, *100*(C7), 13237–13254. https://doi.org/10.1029/95JC00458

Carmack, E., & Chapman, D. C. (2003). Wind-driven shelf/basin exchange on an Arctic shelf: The joint roles of ice cover extent and shelf-break bathymetry: Wind-driven shelf/basin exchange. *Geophysical Research Letters*, *30*(14). https://doi.org/10.1029/2003GL017526

Christiansen, J. S., Mecklenburg, C. W., & Karamushko, O. V. (2014). Arctic marine fishes and their fisheries in light of global change. *Global Change Biology*, *20*(2), 352–359. https://doi.org/10.1111/gcb.12395

Coello-Camba, A., & Agustí, S. (2017). Thermal thresholds of phytoplankton growth in polar waters and their consequences for a warming polar ocean. *Frontiers in Marine Science*, *4*, 168. https://doi.org/10.3389/fmars.2017.00168

Crawford, A. D., Krumhardt, K. M., Lovenduski, N. S., Van Dijken, G. L., & Arrigo, K. R. (2020). Summer high-wind events and phytoplankton productivity in the Arctic Ocean. *Journal of Geophysical Research: Oceans*, *125*(9). https://doi.org/10.1029/2020JC016565

Danabasoglu, G., Deser, C., Rodgers, K., & Timmermann, A. (2023). CESM2 large ensemble. https://doi.org/10.26024/kgmp-c556

Danabasoglu, G., Lamarque, J.-F., Bacmeister, J., Bailey, D. A., DuVivier, A. K., Edwards, J., et al. (2020). The Community Earth System Model version 2 (CESM2). *Journal of Advances in Modeling Earth Systems*, *12*(2), e2019MS001916. https://doi.org/10.1029/2019MS001916

Deser, C., Phillips, A., Bourdette, V., & Teng, H. (2012). Uncertainty in climate change projections: The role of internal variability. *Climate Dynamics*, *38*(3–4), 527–546. https://doi.org/10.1007/s00382-010-0977-x

Divine, L. M., Pearce, T., Ford, J., Solovyev, B., Galappaththi, E. K., Bluhm, B., & Kaiser, B. A. (2021). Protecting the future arctic. *One Earth*, *4*(12), 1649–1651. https://doi.org/10.1016/j.oneear.2021.11.021

DuVivier, A. K., Holland, M. M., Kay, J. E., Tilmes, S., Gettelman, A., & Bailey, D. A. (2020). Arctic and Antarctic sea ice mean state in the community Earth system model version 2 and the influence of atmospheric chemistry. *Journal of Geophysical Research: Oceans*, *125*(8), e2019JC015934. https://doi.org/10.1029/2019JC015934

Elsworth, G. W., Lovenduski, N. S., & McKinnon, K. A. (2021). Alternate history: A synthetic ensemble of ocean chlorophyll concentrations. *Global Biogeochemical Cycles*, *35*(9). https://doi.org/10.1029/2020GB006924

Elsworth, G. W., Lovenduski, N. S., McKinnon, K. A., Krumhardt, K. M., & Brady, R. X. (2020). Finding the fingerprint of anthropogenic climate change in marine phytoplankton abundance. *Current Climate Change Reports*, *6*(2), 37–46. https://doi.org/10.1007/s40641-020-00156-w

Ershova, E., Hopcroft, R., Kosobokova, K., Matsuno, K., Nelson, R. J., Yamaguchi, A., & Eisner, L. (2015). Long-term changes in summer zooplankton communities of the western Chukchi Sea, 1945–2012. *Oceanography*, *28*(3), 100–115. https://doi.org/10.5670/oceanog.2015.60

Eyring, V., Bony, S., Meehl, G. A., Senior, C. A., Stevens, B., Stouffer, R. J., & Taylor, K. E. (2016). Overview of the Coupled Model Intercomparison Project phase 6 (CMIP6) experimental design and organization. *Geoscientific Model Development*, *9*(5), 1937–1958. https://doi.org/10.5194/gmd-9-1937-2016

Falkowski, P. G. (2012). Ocean Science: The power of plankton. *Nature*, *483*(7387), S17–S20. https://doi.org/10.1038/483s17a

Field, C. B., Behrenfeld, M. J., Randerson, J. T., & Falkowski, P. G. (1998). Primary production of the biosphere: Integrating terrestrial and oceanic components. *Science*, *281*(5374), 237–240. https://doi.org/10.1126/science.281.5374.237

Fossheim, M., Primicerio, R., Johannesen, E., Ingvaldsen, R. B., Aschan, M. M., & Dolgov, A. V. (2015). Recent warming leads to a rapid borealization of fish communities in the Arctic. *Nature Climate Change*, *5*(7), 673–677. https://doi.org/10.1038/nclimate2647

Frainer, A., Primicerio, R., Kortsch, S., Aune, M., Dolgov, A. V., Fossheim, M., & Aschan, M. M. (2017). Climate-driven changes in functional biogeography of Arctic marine fish communities. *Proceedings of the National Academy of Sciences*, *114*(46), 12202–12207. https://doi.org/10.1073/pnas.1706080114

Fransner, F., Olsen, A., Årthun, M., Counillon, F., Tjiputra, J., Samuelsen, A., & Keenlyside, N. (2023). Phytoplankton abundance in the Barents Sea is predictable up to five years in advance. *Communications Earth & Environment*, *4*(1), 141. https://doi.org/10.1038/s43247-023-00791-9

Frölicher, T. L., Ramseyer, L., Raible, C. C., Rodgers, K. B., & Dunne, J. (2020). Potential predictability of marine ecosystem drivers. *Biogeosciences*, *17*(7), 2061–2083. https://doi.org/10.5194/bg-17-2061-2020

Germe, A., Chevallier, M., Salas Y Mélia, D., Sanchez-Gomez, E., & Cassou, C. (2014). Interannual predictability of Arctic sea ice in a global climate model: Regional contrasts and temporal evolution. *Climate Dynamics*, *43*(9–10), 2519–2538. https://doi.org/10.1007/s00382-014-2071-2

Hamilton, C., Lydersen, C., Aars, J., Biuw, M., Boltunov, A., Born, E., et al. (2021). Marine mammal hotspots in the Greenland and Barents seas. *Marine Ecology Progress Series*, *659*, 3–28. https://doi.org/10.3354/meps13584

Holland, M. M., & Bailey, D. (2024a). CESM2 perfect model prediction ensembles, 2030. *Research Data Archive at the National Center for Atmospheric Research, Computational and Information Systems Laboratory*. https://doi.org/10.5065/2E1Z-JN83

Holland, M. M., & Bailey, D. (2024b). CESM2 perfect model predictions for 2010. *Research Data Archive at the National Center for Atmospheric Research, Computational and Information Systems Laboratory*. https://doi.org/10.5065/7XEE-S265

Holland, M. M., Bailey, D. A., & Vavrus, S. (2011). Inherent sea ice predictability in the rapidly changing Arctic environment of the Community Climate System Model, version 3. *Climate Dynamics*, *36*(7–8), 1239–1253. https://doi.org/10.1007/s00382-010-0792-4

Holland, M. M., & Bitz, C. M. (2003). Polar amplification of climate change in coupled models. *Climate Dynamics*, *21*(3–4), 221–232. https://doi.org/10.1007/s00382-003-0332-6

Holland, M. M., & Hunke, E. (2022). A review of Arctic sea ice climate predictability in large-scale Earth system models. *Oceanography*. https://doi.org/10.5670/oceanog.2022.113

Holland, M. M., Landrum, L., Bailey, D., & Vavrus, S. (2019). Changing seasonal predictability of arctic summer sea ice area in a warming climate. *Journal of Climate*, *32*(16), 4963–4979. https://doi.org/10.1175/JCLI-D-19-0034.1

Hollowed, A. B., & Sundby, S. (2014). Change is coming to the northern oceans. *Science*, *344*(6188), 1084–1085. https://doi.org/10.1126/science.1251166

Hoover, C., Bailey, M., Higdon, J., Ferguson, S. H., & Sumaila, R. (2013). Estimating the economic value of narwhal and beluga hunts in Hudson Bay, Nunavut. *Arctic*, *66*(1), 1–16. https://doi.org/10.14430/arctic4261

Hopcroft, R. R., Clarke, C., Nelson, R. J., & Raskoff, K. A. (2005). Zooplankton communities of the Arctic?s Canada Basin: The contribution by smaller taxa. *Polar Biology*, *28*(3), 198–206. https://doi.org/10.1007/s00300-004-0680-7

Hunke, E., Lipscomb, W., Jones, P., Turner, A., Jeffery, N., & Elliott, S. (2017). CICE, the los Alamos sea ice model.

Joiris, C. R. (2011). A major feeding ground for cetaceans and seabirds in the South-Western Greenland Sea. *Polar Biology*, *34*(10), 1597–1607. https://doi.org/10.1007/s00300-011-1022-1

Koenigk, T., & Mikolajewicz, U. (2009). Seasonal to interannual climate predictability in mid and high northern latitudes in a global coupled model. *Climate Dynamics*, *32*(6), 783–798. https://doi.org/10.1007/s00382-008-0419-1

Krumhardt, K. M., Lovenduski, N. S., Long, M. C., & Lindsay, K. (2017). Avoidable impacts of ocean warming on marine primary production: Insights from the CESM ensembles. *Global Biogeochemical Cycles*, *31*(1), 114–133. https://doi.org/10.1002/2016GB005528

Krumhardt, K. M., Lovenduski, N. S., Long, M. C., Luo, J. Y., Lindsay, K., Yeager, S., & Harrison, C. (2020). Potential predictability of net primary production in the ocean. *Global Biogeochemical Cycles*, *34*(6). https://doi.org/10.1029/2020GB006531

Kwok, R. (2018). Arctic sea ice thickness, volume, and multiyear ice coverage: Losses and coupled variability (1958–2018). *Environmental Research Letters*, *13*(10), 105005. https://doi.org/10.1088/1748-9326/aae3ec

Lee, Y. J., Matrai, P. A., Friedrichs, M. A. M., Saba, V. S., Antoine, D., Ardyna, M., et al. (2015). An assessment of phytoplankton primary productivity in the Arctic Ocean from satellite ocean color/in situ chlorophyll-*a* based models. *Journal of Geophysical Research: Oceans*, *120*(9), 6508–6541. https://doi.org/10.1002/2015JC011018

Lewis, K. M., & Arrigo, K. R. (2020). Ocean color algorithms for estimating chlorophyll *a*, CDOM absorption, and Particle backscattering in the Arctic Ocean. *Journal of Geophysical Research: Oceans*, *125*(6). https://doi.org/10.1029/2019JC015706

Lewis, K. M., Van Dijken, G. L., & Arrigo, K. R. (2020). Changes in phytoplankton concentration now drive increased Arctic Ocean primary production. *Science*, *369*(6500), 198–202. https://doi.org/10.1126/science.aay8380

Li, W. K., McLaughlin, F. A., Lovejoy, C., & Carmack, E. C. (2009). Smallest algae thrive as the Arctic Ocean freshens. *Science*, *326*(5952), 539. https://doi.org/10.1126/science.1179798

Lindsay, R. W., Zhang, J., Schweiger, A. J., & Steele, M. A. (2008). Seasonal predictions of ice extent in the Arctic Ocean. *Journal of Geophysical Research*, *113*(C2), 2007JC004259. https://doi.org/10.1029/2007JC004259

Loeng, H., Brander, K., Carmack, E., Denisenko, S., Drinkwater, K., Hansen, B., et al. (2005). CH. 9. Marine systems. In *Arctic climate impact assessment*.

Logerwell, E., Busby, M., Carothers, C., Cotton, S., Duffy-Anderson, J., Farley, E., et al. (2015). Fish communities across a spectrum of habitats in the western Beaufort Sea and Chukchi Sea. *Progress in Oceanography*, *136*, 115–132. https://doi.org/10.1016/j.pocean.2015.05.013

Long, M. C., Lindsay, K., & Holland, M. M. (2015). Modeling photosynthesis in sea ice-covered waters: Photosynthesis in sea ice-covered waters. *Journal of Advances in Modeling Earth Systems*, *7*(3), 1189–1206. https://doi.org/10.1002/2015MS000436

Long, M. C., Moore, J. K., Lindsay, K., Levy, M., Doney, S. C., Luo, J. Y., et al. (2021). Simulations with the Marine Biogeochemistry Library (MARBL). *Journal of Advances in Modeling Earth Systems*, *13*(12), e2021MS002647. https://doi.org/10.1029/2021MS002647

Lysenko, D., & Schott, S. (2019). Food security and wildlife management in Nunavut. *Ecological Economics*, *156*, 360–374. https://doi.org/10.1016/j.ecolecon.2018.10.008

McIlhattan, E. A., Kay, J. E., & L'Ecuyer, T. S. (2020). Arctic clouds and precipitation in the community Earth system model version 2. *Journal of Geophysical Research: Atmospheres*, *125*(22), e2020JD032521. https://doi.org/10.1029/2020JD032521

McLaughlin, F. A., & Carmack, E. C. (2010). Deepening of the nutricline and chlorophyll maximum in the Canada Basin interior, 2003–2009. *Geophysical Research Letters*, *37*(24). https://doi.org/10.1029/2010GL045459

Meier, W., & Stroeve, J. (2022). An updated assessment of the changing Arctic sea ice cover. *Oceanography*, *35*(3/4). https://doi.org/10.5670/oceanog.2022.114

Merryfield, W. J., Lee, W.-S., Wang, W., Chen, M., & Kumar, A. (2013). Multi-system seasonal predictions of Arctic sea ice. *Geophysical Research Letters*, *40*(8), 1551–1556. https://doi.org/10.1002/grl.50317

Mueter, F. J., Planque, B., Hunt, G. L., Alabia, I. D., Hirawake, T., Eisner, L., et al. (2021). Possible future scenarios in the gateways to the arctic for subarctic and arctic marine systems: II. Prey resources, food webs, fish, and fisheries. *ICES Journal of Marine Science*, *78*(9), 3017–3045. https://doi.org/10.1093/icesjms/fsab122

Munk, P. (2003). Changes in plankton and fish larvae communities across hydrographic fronts off West Greenland. *Journal of Plankton Research*, *25*(7), 815–830. https://doi.org/10.1093/plankt/25.7.815

Nummelin, A., Li, C., & Smedsrud, L. H. (2015). Response of Arctic Ocean stratification to changing river runoff in a column model. *Journal of Geophysical Research: Oceans*, *120*, 2655–2675. https://doi.org/10.1002/2014JC010571.Received

Oliver, H., McGillicuddy, D. J., Krumhardt, K. M., Long, M. C., Bates, N. R., Bowler, B. C., et al. (2023). Environmental drivers of coccolithophore growth in the Pacific sector of the Southern Ocean. *Global Biogeochemical Cycles*, *37*(11), e2023GB007751. https://doi.org/10.1029/2023GB007751

Payne, C. M., Van Dijken, G. L., & Arrigo, K. R. (2024). Pan-Arctic analysis of the frequency of under-ice and marginal ice zone phytoplankton blooms, 2003–2021. *Elem Sci Anth*, *12*(1), 00076. https://doi.org/10.1525/elementa.2023.00076

Pohlmann, H., Botzet, M., Latif, M., Roesch, A., Wild, M., & Tschuck, P. (2004). Estimating the decadal predictability of a coupled AOGCM. *Journal of Climate*, *17*(22), 4463–4472. https://doi.org/10.1175/3209.1

Rainville, L., & Woodgate, R. A. (2009). Observations of internal wave generation in the seasonally ice-free Arctic. *Geophysical Research Letters*, *36*(23), L23604. https://doi.org/10.1029/2009GL041291

Rantanen, M., Karpechko, A. Y., Lipponen, A., Nordling, K., Hyvärinen, O., Ruosteenoja, K., et al. (2022). The Arctic has warmed nearly four times faster than the globe since 1979. *Communications Earth & Environment*, *3*(1), 168. https://doi.org/10.1038/s43247-022-00498-3

Rodgers, K. B., Lee, S.-S., Rosenbloom, N., Timmermann, A., Danabasoglu, G., Deser, C., et al. (2021). Ubiquity of human-induced changes in climate variability. *Earth System Dynamics*, *12*(4), 1393–1411. https://doi.org/10.5194/esd-12-1393-2021

Rysgaard, S., Nielsen, T., & Hansen, B. (1999). Seasonal variation in nutrients, pelagic primary production and grazing in a high-Arctic coastal marine ecosystem, Young Sound, Northeast Greenland. *Marine Ecology Progress Series*, *179*, 13–25. https://doi.org/10.3354/meps179013

Screen, J. A., & Simmonds, I. (2010). The central role of diminishing sea ice in recent Arctic temperature amplification. *Nature*, *464*(7293), 1334–1337. https://doi.org/10.1038/nature09051

Séférian, R., Berthet, S., & Chevallier, M. (2018). Assessing the decadal predictability of Land and ocean carbon uptake. *Geophysical Research Letters*, *45*(5), 2455–2466. https://doi.org/10.1002/2017GL076092

Séférian, R., Bopp, L., Gehlen, M., Swingedouw, D., Mignot, J., Guilyardi, E., & Servonnat, J. (2014). Multiyear predictability of tropical marine productivity. *Proceedings of the National Academy of Sciences*, *111*(32), 11646–11651. https://doi.org/10.1073/pnas.1315855111

Sigman, D. M., & Hain, M. P. (2012). The biological productivity of the ocean. *Nature Education*, *3*(6).

Smidt, E. L. B. (1979). *Annual cycles of primary production and of zooplankton at Southwest Greenland: With figures of some bottom invertebrate larvae* (Vol. 1). Commission for Scientific Research in Greenland.

Tagliabue, A., Kwiatkowski, L., Bopp, L., Butenschön, M., Cheung, W., Lengaigne, M., & Vialard, J. (2021). Persistent uncertainties in ocean net primary production climate change projections at regional scales raise challenges for assessing impacts on ecosystem services. *Frontiers in Climate*, *3*, 738224. https://doi.org/10.3389/fclim.2021.738224

Tai, T. C., Steiner, N. S., Hoover, C., Cheung, W. W., & Sumaila, U. R. (2019). Evaluating present and future potential of arctic fisheries in Canada. *Marine Policy*, *108*, 103637. https://doi.org/10.1016/j.marpol.2019.103637

Terhaar, J., Kwiatkowski, L., & Bopp, L. (2020). Emergent constraint on Arctic Ocean acidification in the twenty-first century. *Nature*, *582*(7812), 379–383. https://doi.org/10.1038/s41586-020-2360-3

Timmermans, M. L., & Labe, Z. (2023). NOAA arctic report card 2023: Sea surface temperature. https://doi.org/10.25923/E8JC-F342

Tommasi, D., Stock, C. A., Pegion, K., Vecchi, G. A., Methot, R. D., Alexander, M. A., & Checkley, D. M. (2017). Improved management of small pelagic fisheries through seasonal climate prediction. *Ecological Applications*, *27*(2), 378–388. https://doi.org/10.1002/eap.1458

Tremblay, J.-É., Bélanger, S., Barber, D. G., Asplin, M., Martin, J., Darnis, G., et al. (2011). Climate forcing multiplies biological productivity in the coastal Arctic Ocean. *Geophysical Research Letters*, *38*(18). https://doi.org/10.1029/2011GL048825

Tsujii, K., Otsuki, M., Akamatsu, T., Matsuo, I., Amakasu, K., Kitamura, M., et al. (2016). The migration of fin whales into the southern Chukchi Sea as monitored with passive acoustics. *ICES Journal of Marine Science*, *73*(8), 2085–2092. https://doi.org/10.1093/icesjms/fsv271

Vancoppenolle, M., Bopp, L., Madec, G., Dunne, J., Ilyina, T., Halloran, P. R., & Steiner, N. (2013). Future Arctic Ocean primary productivity from CMIP5 simulations: Uncertain outcome, but consistent mechanisms: Future arctic ocean primary productivity. *Global Biogeochemical Cycles*, *27*(3), 605–619. https://doi.org/10.1002/gbc.20055

Volk, T., & Hoffert, M. I. (1985). Ocean carbon pumps: Analysis of relative strengths and efficiencies in Ocean-driven atmospheric CO_2 changes. In E. Sundquist & W. Broecker (Eds.), *The carbon cycle and atmospheric CO_2: Natural variations archean to present* (Vol. 32, pp. 99–110). American Geophysical Union. https://doi.org/10.1029/GM032p0099

Webster, M. A., DuVivier, A. K., Holland, M. M., & Bailey, D. A. (2021). Snow on Arctic sea ice in a warming climate as simulated in CESM. *Journal of Geophysical Research: Oceans*, *126*(1). https://doi.org/10.1029/2020JC016308

Westberry, T., Behrenfeld, M. J., Siegel, D. A., & Boss, E. (2008). Carbon-based primary productivity modeling with vertically resolved photoacclimation. *Global Biogeochemical Cycles*, *22*(2), 2007GB003078. https://doi.org/10.1029/2007GB003078

Wisz, M. S., Broennimann, O., Grønkjær, P., Møller, P. R., Olsen, S. M., Swingedouw, D., et al. (2015). Arctic warming will promote Atlantic–Pacific fish interchange. *Nature Climate Change*, *5*(3), 261–265. https://doi.org/10.1038/nclimate2500

Xu, A., Jin, M., Wu, Y., & Qi, D. (2023a). Response of nutrients and primary production to high wind and upwelling-favorable wind in the Arctic Ocean: A modeling perspective. *Frontiers in Marine Science*, *10*, 1065006. https://doi.org/10.3389/fmars.2023.1065006

Xu, L., Yu, H., Chen, Z., Du, W., Chen, N., & Zhang, C. (2023b). Monthly Ocean primary productivity forecasting by joint use of seasonal climate prediction and temporal memory. *Remote Sensing*, *15*(5), 1417. https://doi.org/10.3390/rs15051417

Yeager, S. G., Danabasoglu, G., Rosenbloom, N. A., Strand, W., Bates, S. C., Meehl, G. A., et al. (2018). Predicting near-term changes in the Earth system: A large ensemble of initialized decadal prediction simulations using the community Earth system model. *Bulletin of the American Meteorological Society*, *99*(9), 1867–1886. https://doi.org/10.1175/BAMS-D-17-0098.1

Yeager, S. G., Rosenbloom, N., Glanville, A. A., Wu, X., Simpson, I., Li, H., et al. (2022). The Seasonal-To-Multiyear Large Ensemble (SMYLE) prediction system using the community Earth system model version 2. *Geoscientific Model Development*, *15*(16), 6451–6493. https://doi.org/10.5194/gmd-15-6451-2022

Zeller, D., Booth, S., Pakhomov, E., Swartz, W., & Pauly, D. (2011). Arctic fisheries catches in Russia, USA, and Canada: Baselines for neglected ecosystems. *Polar Biology*, *34*(7), 955–973. https://doi.org/10.1007/s00300-010-0952-3

Zhang, X., Walsh, J. E., Zhang, J., Bhatt, U. S., & Ikeda, M. (2004). Climatology and interannual variability of arctic cyclone activity: 1948–2002. *Journal of Climate*, *17*(12), 18–2317. https://doi.org/10.1175/1520-0442(2004)017<2300:caivoa>2.0.co;2